Supporting Information

Engineering Plasticization Resistant Gas Separation Membranes Using Metal-Organic Nanocapsules

Hongliang Wang[1], Kexin Zhang[1], Jerry Pui Ho Li[1,4], Jingyu Huang[2], Biao Yuan[1], Chen Zhang[3], Yi Yu[1], Yong Yang[1], Yongjin Lee[1], Tao Li[1]*

[1] School of Physical Science and Technology, ShanghaiTech University, Shanghai 201210, China

[2] Department of Materials Science & Engineering, University of California, Berkeley, California 94720, United States

[3] Department of Chemical and Biomolecular Engineering, North Carolina State University, Raleigh, North Carolina 27695, United States

[4] School of Chemistry and Chemical Engineering, Queen's University Belfast, Belfast, BT9 5AG, UK

*Corresponding author: litao1@shanghaitech.edu.cn

This file includes:

Section S1. Materials

All reagents and solvents obtained were used without further purification unless otherwise specified. Pyrogallol (purity ≥ 99%), butyraldehyde (purity ≥ 97%), hexanal (purity ≥97%), octanal (purity ≥ 97%), decanal (purity ≥ 97%), tetrafluoroterephthalonitrile (TFTPN, purity of 99%), pyridine (ACS grade, ≥ 99%), N,N-Dimethylformamide (DMF, GC grade, > 99.9%), potassium carbonate (ACS grade, ≥ 99.0%) trimethylamine (TEA, AR grade, purity 99%), 1-Methyl-2-pyrrolidinone (NMP, AR grade, purity > 99%) were purchased from Aladdin Reagent Company (Shanghai, China). 2,4,6-trimethyl-1,3-phenylenediamine (DAM, purity 98%), were purchased from Adamas Reagent. 2,3,5,6-Tetramethyl-1,4-phenylenediamine (durene, purity ≥ 98%), 4,4'-(Hexafluoroisopropylidene) diphthalic anhydride (6FDA, purity 98%) were purchased from TCI. $Cu(NO_3)_2 \cdot 3H_2O$ (AR grade, purity of 99%), concentrated hydrochloric acid (AR grade, 37%), acetic anhydride (AR grade, purity ≥ 98.5%) were purchased from Hushi Laboratorial Equipment Co., Ltd. (Shanghai, China). 5,5'-Tetrahydroxy-3,3,3',3'-tetramethyl spirobisindane (TTSBI, purity of 97%) was purchased from Alfa Aesar. Acetone (AR grade, purity ≥ 99.5%) was purchased from Greagent (Shanghai, China). NMP was heated under reflux for four hours over calcium hydride for desiccation before distillation. Fresh anhydrous DMF was obtained by a Vigor solvent purification system before use. 6FDA was purified by recrystallization from acetic anhydride. DAM and Durene were purified by recrystallization from ethanol. TTSBI was purified from hot methanol by dichloromethane. TFTPN was recrystallized *via* vacuum sublimation at 140 °C. Anhydrous K_2CO_3 was ground, heated under vacuum at 110 ºC before use.

Section S2. Synthesis

Synthesis of C-alkylpyrogallol[4]arene (PgC_n)

PgC_n (n=3, 5, 7, 9) were synthesized through a condensation reaction between pyrogallol and an aldehyde catalyzed by concentrated hydrochloric acid[1]. Taking PgC_5 as an example, a solution of pyrogallol (10 g, 80 mmol) in methanol (40 ml) was mixed with hexanal (9.84 ml, 80 mmol) followed by adding 3.5 ml of concentrated HCl. The mixture was then refluxed at 110 °C for 24 hours during which time the color of the solution changed from colorless to deep red. After cooling down to room temperature, the precipitate was collected by centrifugation and washed by fresh methanol three times. PgC_5 was collected and dried under vacuum affording a white solid.

Synthesis of PgC_nCu nanocapsules

In a typical synthesis of hexameric PgC_nCu nanocapsules, the PgC_n macrocycles (n=3, 5, 7, 9) were reacted with $Cu(NO_3)_2 \cdot 3H_2O$ in acetone using pyridine (py) as a modulator. PgC_n (n= 3, 5, 7 and 9, 1 mmol) was added to an acetone (10 ml)-pyridine (0.645 ml, 8 mmol) mixture to form a ligand stock solution. $Cu(NO_3)_2 \cdot 3H_2O$ (966.40 mg, 4 mmol) was added to acetone (10 ml) to form a metal ion stock solution. The two stock solutions were then mixed in a beaker and sonicated to give a dark reddish-brown mixture. PgC_nCu crystals were precipitated upon addition of deionized water (50 ml) and collected through centrifugation. The red powder products were then washed by methanol several times and dried in vacuum for future use.

Synthesis of 6FDA-DAM polyimide[2]

DAM (2.152 g,14.33 mmol) and NMP (15 ml) were added into a 100 ml flask equipped with a nitrogen inlet. The mixture was cooled to 0 ºC and then 6FDA (6.364 g, 14.33 mmol) and NMP (15 ml) were added. The solution was stirred for 24 hours to form polyamic acid. Next, 2 ml of trimethylamine (TEA), 5.4 ml of acetic anhydride (Ac_2O) and NMP (6 ml) were added. The mixture was vigorously stirred for 20 hours to allow complete imidization. The polyimide product was precipitated in methanol (1 L), filtered, washed with fresh methanol several times and dried under vacuum at 150 ºC for 24 hours.

Synthesis of 6FDA-durene polyimide

Durene (2.354 g,14.33 mmol) and NMP (26 ml) were added into a 250 ml flask equipped with a nitrogen inlet. The mixture was cooled to 0 ºC and then 6FDA (6.364 g, 14.33 mmol) and NMP (26 ml) were added. The solution was stirred for 24 hours to form polyamic acid. Next, 2 ml of TEA, 5.4 ml of Ac_2O and NMP (10 ml) were added. The mixture was vigorously stirred for 20 hours to allow complete imidization. The polyimide product was precipitated in methanol (1 L), filtered, washed with methanol several times and dried under vacuum at 150 ºC for 24 hours.

Synthesis of PIM-1

PIM-1 was synthesized *via* low-temperature condensation between TTSBI and TFTPN according to a reported protocol[3]. A mixture of TTSBI (10.213 g, 30 mmol), TFTBN (6.003 g, 30 mmol), anhydrous K_2CO_3 (8.292 g, 60 mmol) and anhydrous DMF

(200 ml) were stirred 15 minutes with a nitrogen inlet to ensure that all monomers were dissolved. Then the mixture was vigorously stirred for 23 hours at 55 ºC. After cooling to room temperature, PIM-1 was precipitated in water. The crude product was then re-dissolved in chloroform and precipitated in methanol. The procedure was repeated for three times to ensure complete removal of impurities. Finally, the yellow powder was dried under vacuum at 150 ºC for 24 hours.

Membranes fabrication

To fabricate neat polymer membranes, the polymers (PC, CA, PMMA, PSF, 6FDA-durene, 6FDA-DAM, PIM-1, PVP and PLA) were first dissolved in $CHCl_3$ and probe sonicated for several minutes. The polymer solutions (10 wt%) were filtered through a 0.45 micron PTFE syringe filter and then casted onto a flat quartz plate. After slow evaporation of solvents, membranes were peeled off from the quartz plate and dried overnight.

To fabricate PgC_nCu-polymer composite membranes, MONCs (0.5, 1, 2, 3 and 5 wt%) were mixed in 10 wt% polymer solutions to form mixture solutions. Ultrasonication was used to assist the complete dissolution of MONCs. It was worth mentioning that there was no obvious viscosity difference between polymer solutions and mixture solutions. The mixture solutions were then filtered through a PTFE syringe filter (0.45 μm) before casting onto a flat quartz plate. After slow evaporation of solvents, membranes were peeled off from the quartz plate and dried overnight. Membranes thicknesses were in the range of 60-80 μm measured by a micrometer.

Section S3. Characterization

SEM images were obtained by JSM 7800F Prime field-emission scanning electron microscope. Samples were coated with Au for 20 seconds using an SBC-12 sputter coater.

For ultramicrotomy, composite membranes were stained by a 0.5wt% RuO_4 water solution to enhance the contrast of the film edge. Then the membranes were embedded into an epoxy resin matrix (EPON 812, Sigma Aldrich) and cured at 60 ºC for 24 hours. The resin pellet was then microtomed into 20 nm slices using a Leica EM UC7 ultramicrotome. The slices were picked up by a nickel TEM grid for imaging.

HAADF-STEM images of PgC_5Cu nanocapsules were taken on a JEM-ARM300F field-emission transmission electron microscope with voltage set at 300 kV. The EDS mapping was performed on a JEM-F200 TEM.

N_2 and CO_2 adsorption isotherms were collected on a BELSORP-max (MicrotracBEL II Corp.). Prior to analyses, samples were activated under vacuum for 12 hours at 120 ºC. The THF vapor adsorption was performed on a MicrotracBELSorp-Aqua adsorption apparatus. The THF solvents were degassed through at least three freeze-pump-thaw cycles before data collection. FTIR spectra were performed on a PerkinElmer FTIR Spectrometer in transmission mode in the range of 4000-500 cm^{-1}. The film sample was uniformly coated on a transparent flat KBr crystal by spin-coating.

The *in-situ* FTIR analysis was performed using a Bruker Vertex 70 (MCT detector) with an aperture opening 4 mm, resolution of 4 cm^{-1}, 200 scans per spectrum (Background: 1000 scans per spectrum), and a scan frequency of 160 kHz. The sample is placed in a

purpose-built in-situ FTIR transmission cell which has been have been detailed elsewhere[4]. For the analysis the PgC_5Cu-PMMA composites, first, take background scan of un-activated PgC_5Cu-PMMA composite. Then *in-situ* activation was carried out at 200 ºC under argon flow for 3 hours. After cooling down to room temperature, the sample scan was conducted.

^1H NMR spectra were recorded on a Bruker AVANCE III HD 400MHz spectrometer.

TGA experiments were performed on a PerkinElmer TGA 8000 at 10 ºC/min under N_2 atmosphere.

Measurement of the Swelling Profiles: The casted thin film was placed in a 125 mL top-capped glass vial. The film thickness was measured using a white-light interferometer (Filmetrics F20). The swelling profile of the film was measured at 23 °C by injecting 500 μL of chloroform into the closed vial. The swelling film thickness under chloroform vapor environment was monitored in situ with Filmetrics F20. After 30 min (or whatever time shown in the chart), the vial was open, and the film was removed from the vial.

DLS experiments were performed in a Malvern zetasizer Nano ZS. In general, the mixture solution was stirred for 24 hours, filtered through a PTFE syringe filter (0.45 μm), and three consecutive measurements were performed for each sample.

Tensile testing was carried out on Instron 5960 at a pulling rate of 2 mm/min. The membrane samples were cut into rectangle-shape with 40 mm × 4 mm, and at least three specimens were tested for each experiment.

DMA was performed on DMA 8000 (PerkinElmer Instruments Inc.) and Q800 (TA

Instruments) with heat rate of 3 ºC/min and frequency of 1 Hz.

Dissolution test

Time-dependent dissolution profiles for neat PC and their composite membranes were obtained by immersing the corresponding membranes in DCM for various time. The remaining membranes were dried under vacuum at 80 ºC for 2 hours. The weight of the membranes was recorded before (W_1) and after (W_2) the dissolution test. The percentages of the insoluble part and soluble part were calculated as follows:

$$\text{Insoluble part } (\%) = \frac{W2}{W1}$$

Soluble part (%) = 100% - insoluble part (%)

The amounts of PgC_5Cu in the supernatant and residual membrane were individually quantified. Taking PC(1) as an example, after immersing PC(1) in DCM for 24 hours, the supernatant and the residual membrane were separated into two test tubes and individually dried. Then, DMF was added into each test tube (1 ml) to dissolve the residual solids. Note that the residual membrane was not soluble in DMF at room temperature. Instead, half an hour heating at 120 ºC was necessary to achieve complete dissolution. The relative quantity of PgC_5Cu was determined by their UV-Vis spectra. The absorption value at 540 nm was used for quantification.

Investigations of PSF/MONC using Molecular Dynamics Simulations

Construction of PSF polymer

With a phenylene sulfone as a repeating unit, a random PSF chain having 10 units was generated within the Materials Studio 7.0[5], as shown in Supplementary Figure 14. Atomic

charges of PSF were estimated based on a phenylene sulfone repeating unit and extended to PSF. This approach is based on the assumption that the atomic charges of a phenylene sulfone unit would not be varied much when a polymer is constructed, except atoms that connected to linkage hydrogens. The atomic charges for a phenylene sulfone unit were obtained by fitting them to the electrostatic potential (ESP) using the Restrained Electrostatic Potential (RESP) method[6]. Structural relaxation were performed using the density functional theory (DFT) within the Gaussian 09[7] at B3LYP 6311g++(d,p) level. Next, do ESP calculation using the same DFT theory and same basis set. Then, the atomic charges were mapped to PSF polymer while adjusting atomic charges bonded to linkage atoms so that a polymer becomes neutral. For a polymer, atom types and their charges are summarized in Supplementary Table 3.

Construction of MONCs

A MONC was constructed with combining six PgC_n units and 24 Cu^{2+} ions, where n is the length of the associated alkyl tail. To obtain atomic charges for PgC_nCu, first, we calculated atomic charges in PgC_1Cu using density functional theory (DFT) calculations that performed within the GGA of Perdew, Burke, and Ernzerhof (PBE)[8]. The Vienna Ab initio Simulation Package (VASP) code[9] with a plane-wave basis set and projector-augmented-wave pseudopotentials[10] was used. PgC_1Cu was relaxed until the energy changed by less than 1×10^{-4} eV and until the residual forces are found to be less than 0.01 eV/°A. For DFT relaxed structure, atomic charges were estimated by using a Bader analysis[11]. Then, for PgC_nCu from n = 3 to 9, atomic charges in the alkyl chain were adopted

from those of the corresponding alkane molecule obtained using the RESP method based on ESP from Gaussian 09 calculations, while atomic charges for non-alkyl chain part were retained from PgC_1Cu. For charge neutrality of PgC_nCu, atomic charges for C and H atoms at the connection point in alkyl chain were further adjusted (see Supplementary Figure 15). Supplementary Table 4 summarizes atom types and their charges for PgC_nCu.

Molecular Dynamics Simulation

To construct a simulation cell for molecular dynamic (MD) simulations, first, we prepared a cubic box of 100nm×100nm×100nm containing 24 PSF chains and one PgC_nCu at the center of the box. Then, with periodic boundary conditions in all directions, the simulation cell was relaxed by performing MD runs using the LAMMPS (Large-scale Atomic/Molecular Massively Parallel Simulator)[12] with a canonical ensemble (NVT) with a timestep of 0.5 fs. During relaxation, box sizes were adjusted so that the final dimensions of each box became 6nm×6nm×6nm. The General Amber Force field (GAFF2.1[13]) was employed to describe interatomic interactions for both PSF and alkyl chains in PgC_nCu while the non-alkyl chain part including in PgC_nCu was treated as rigid. In our calculations, the van der Waals and Coulombic interactions were subject to a 14 Å cutoff. To describe pairwise interactions between Cu in PgC_nCu and O in the sulfonyl group of PSF, we applied the Buckingham potential with parameters from Woodley et al.'s work[14]. Considering that our initial PSF configuration is random, to facilitate formation of a coordination bonding between Cu and O in PSF to be observed in reasonable MD simulation time scale, during our MD, a bond is created with the equilibrium bond length of 2.2 Å when a Cu and O

pairwise distance is less than 2.4 Å, but deleted when the distance becomes longer than 2.5 Å. For each Cu atom, only one coordination bonding was allowed to be formed. To minimize the effect of this artifact on MD dynamics, force constant parameter (k) in the harmonic bond model for was set as 5 kcal/mole Å^2 which is about two order magnitude smaller compared to that for other bond types.

To obtain the equilibrated configuration of each PgC_nCu/PSF system, we performed relaxation procedures consisted of a total of 8 ns with four cycles of two consecutive MD simulations (each simulation for 1 ns) at different temperatures; 1) NVT at 800 K and 2) NVT at 400 K. After equilibration steps, follow-up 2 ns MD runs at 300 K were performed to obtain the final configuration for PgC_nCu/PSF system.

Gas permeation measurements

The single gas permeation of newly designed MONCs containing hybrids membranes and neat polymer membranes were measured at 35 ºC with a home-built variable-pressure constant-volume setup. The pre-activated films were placed on the central hole of a custom-made brass disk sealed by heat-resist epoxy resin to prepare of film modules. In a typical permeation measurement procedure, the film module was installed in the membrane cell, and then upstream and downstream were evacuated at least 1 hours. Before measuring, the leak rate of downstream was measured. Single point permeation was performed at a feed pressure of 2.8 atm and temperature of 35 ºC. High pressure single gas permeation experiment of C_2H_6, C_2H_4, CH_4 and CO_2 was performed over the pressure range between 2.8 and highest achievable gas pressure. The permeability coefficient of each gas was

calculated according to the following equation:

$$P = \frac{lV_{cell}}{A\Delta_p RT}[(dp/dt)_{SS} - (dp/dt)_{leak}]$$

Where P is the permeability coefficient (1 barrer = 10^{-10} cc(STP) cm $cm^{-2}s^{-1}cmHg^{-1}$), l is the thickness of the film, A is the effective area of the membrane, V_{cell} is the downstream volume, T is the operating temperature in kelvin, $(dp/dt)_{SS}$ is the steady-state permeation rate, and $(dp/dt)_{leak}$ is the leak rate. Δp is the pressure difference between upstream and downstream. R is the gas constant.

At high pressure, non-ideal gas-phase behavior needs to be considered. Thus, gas fugacity (f) was calculated to provide a more accurate measure of permeability. The fugacity-based permeability was calculated as following equation:

$$P = \frac{lV_{cell}}{AfRT}[(dp/dt)_{SS} - (dp/dt)_{leak}]$$

Where f is the fugacity of the feed. The fugacities were estimated from the virial equation including second and third virial coefficients at 35 ºC.[15]

The ideal selectivity of pure gas A and B can be calculated by using the following equation:

$$\alpha = \frac{P_A}{P_B}$$

where P_A and P_B is the permeability coefficient of pure gas A and B, respectively.

The upper bound lines for polymer membranes are drawn according to references[16-18].

Physical aging of the neat 6FDA-DAM and 6FDA-DAM(2) were studied for a period of 42 days. The aging tests were conducted on CH_4 and CO_2 at 35 ºC, an upstream pressure of 2.8 atm. When not being tested, membranes were aged at room temperature in a moisture

proof box with desiccant to isolate membranes from humid air.

Section S4. Supplemental figures and tables

Figures

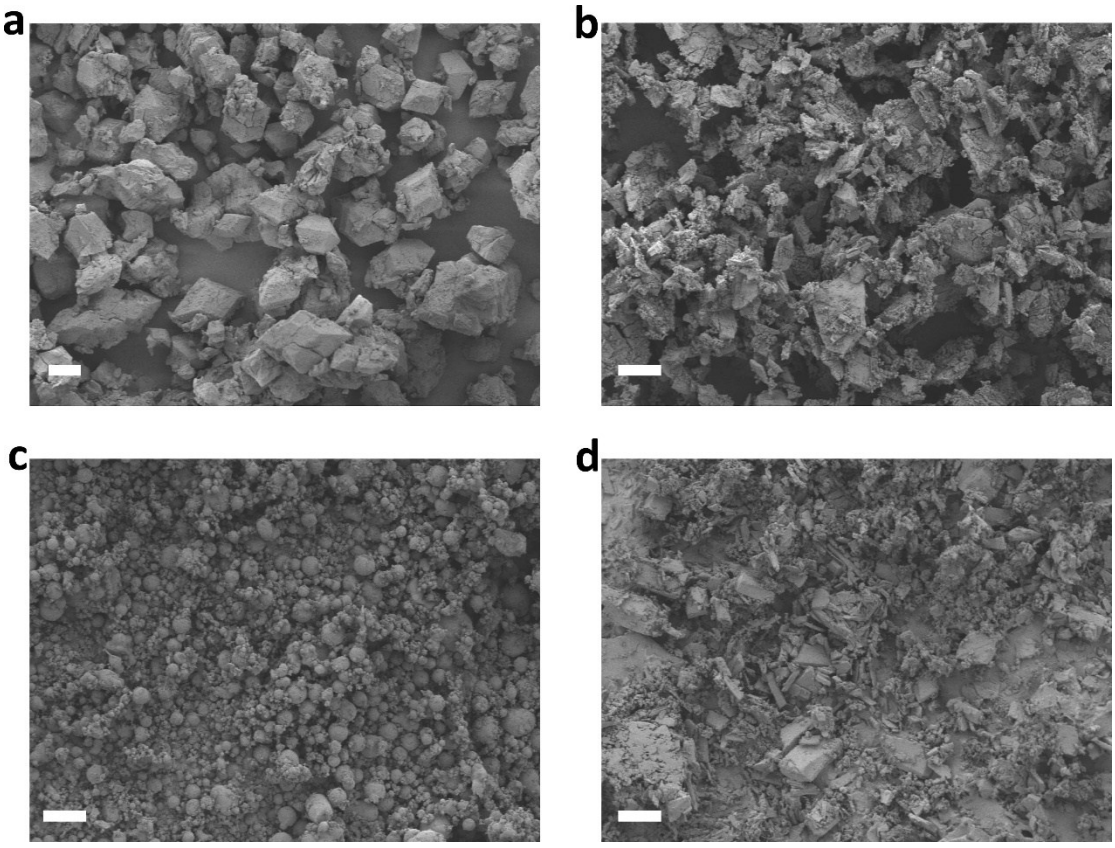

Figure S1. SEM images of as-synthesized PgC_3Cu (a), PgC_5Cu (b), PgC_7Cu (c), PgC_9Cu (d), Scale bar 10 μm.

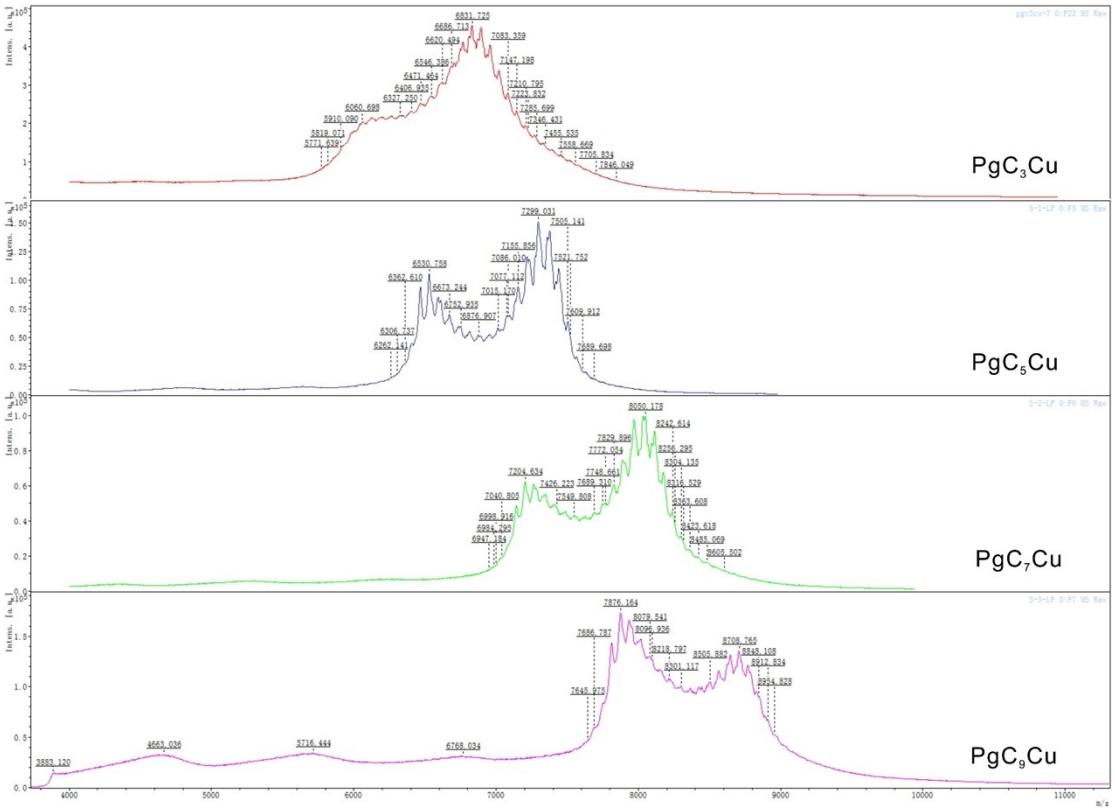

Figure S2. MALDI-TOF spectra of PgC_3Cu, PgC_5Cu, PgC_7Cu and PgC_9Cu.

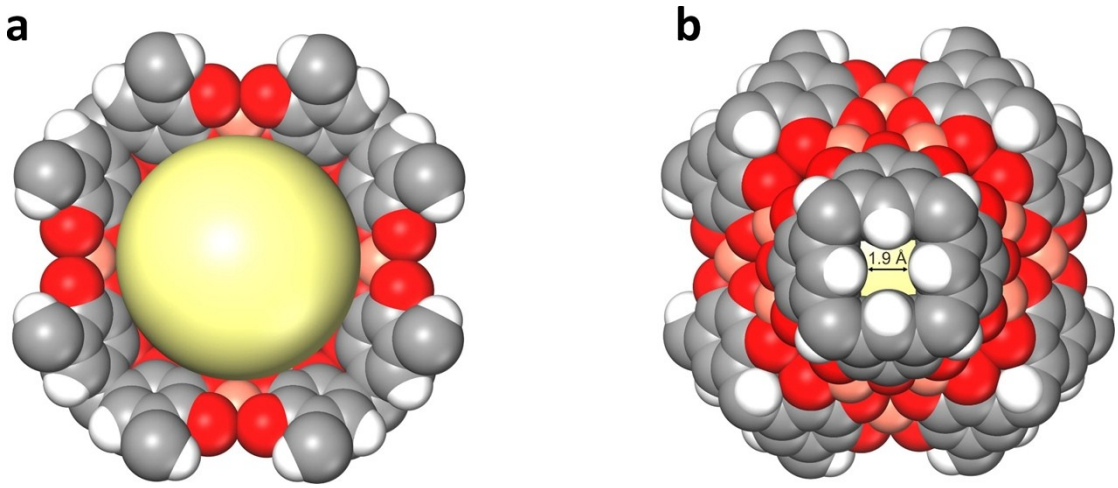

Figure S3. Space-filling representation of cavity (a) and aperture size (b) in PgC_nCu. Cu = pink, C = grey, O = red, and H = white.

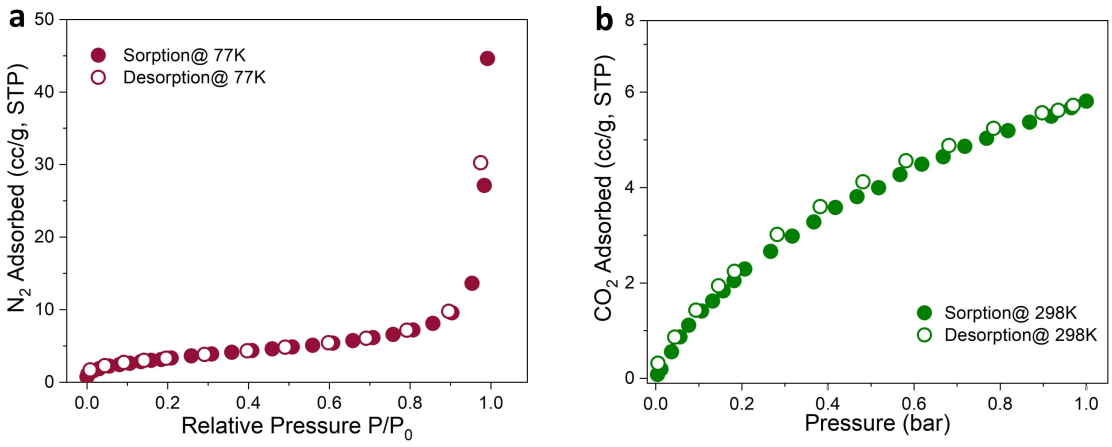

Figure S4. Nitrogen isotherm (a) and carbon dioxide (b) isotherm of PgC_5Cu nanocapsules.

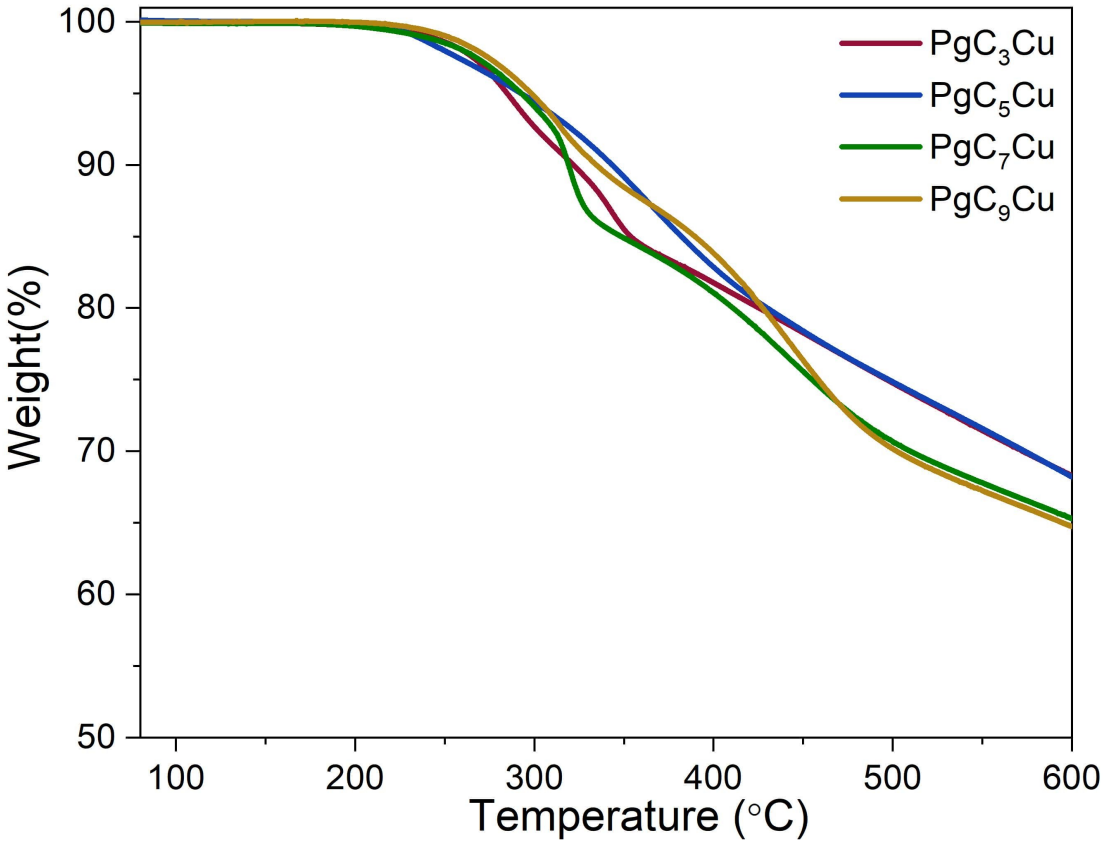

Figure S5. TGA curves of PgC_nCu (n=3,5,7,9) nanocapsules in the N_2 atmosphere with a ramping rate of 10 °C/min.

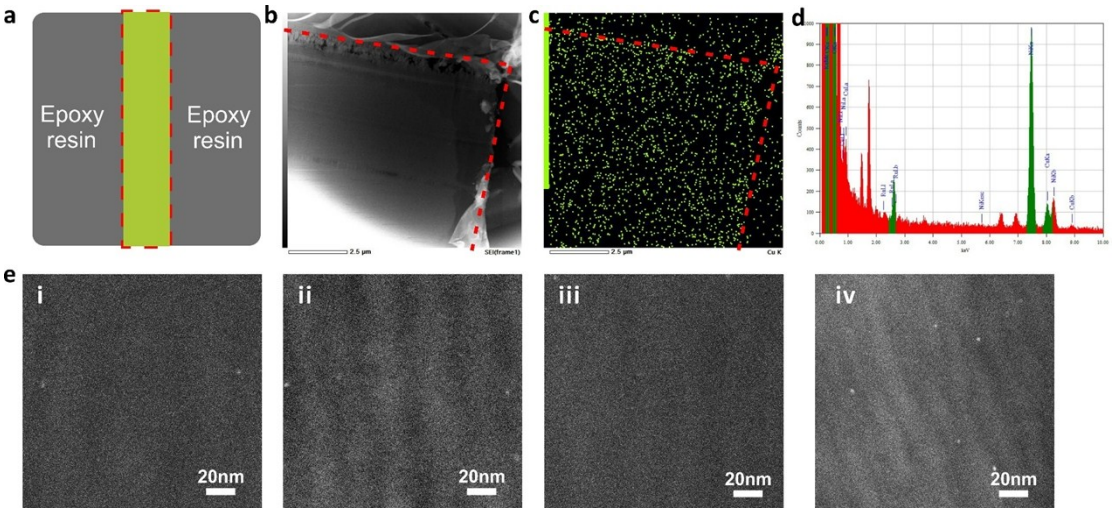

Figure S6. (a) scheme of sample film (green) embedded in epoxy resin. (b) The TEM image of a 20 nm slice of 6FDA-DAM(2). The bright region in lower left corner is caused by large angle scanning electron beam at low magnification. (c) STEM-EDS elemental mapping of Cu in 6FDA-DAM(2). (d) The EDS spectrum of 6FDA-DAM(2). (e) Representative STEM images of randomly selected area of a 20 nm thick 6FDA-DAM(2) slice. The white dots represent occasional agglomerations (< 3.5 nm) of PgC_5Cu in the polymer matrix.

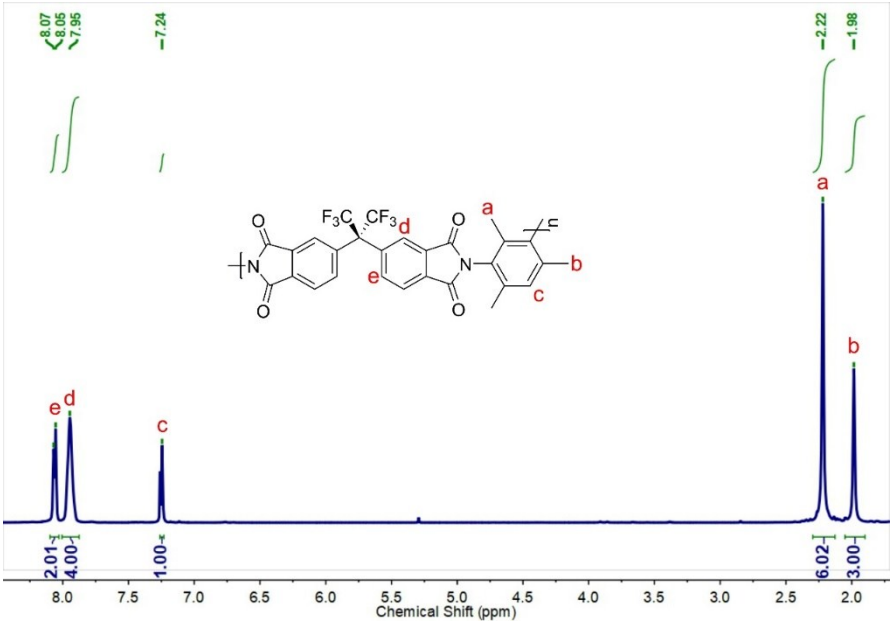

Figure S7. ^{1}H NMR spectrum of neat 6FDA-DAM. ^{1}H NMR (400 MHz, $CDCl_3$), 8.05-8.07 (d, 2H), 7.91-8.01 (m, 4H), 7.24 (s, 1H), 2.22 (s, 6H), 1.98 (s, 3H).

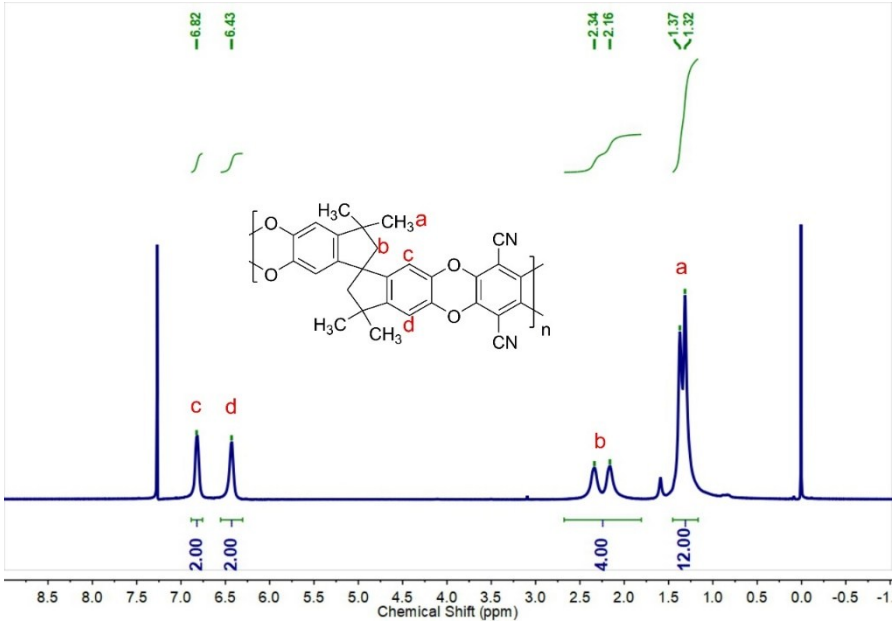

Figure S8. ^{1}H NMR spectrum of PIM-1. The peak at 7.26 and 0 ppm corresponding to $CDCl_3$ and tetramethylsilane (TMS). ^{1}H NMR (400 MHz, $CDCl_3$), 6.82 (s, 2H), 6.43 (s, 2H), 2.16 -2.34 (d, 4H), 1.32 - 1.37(d, 12H).

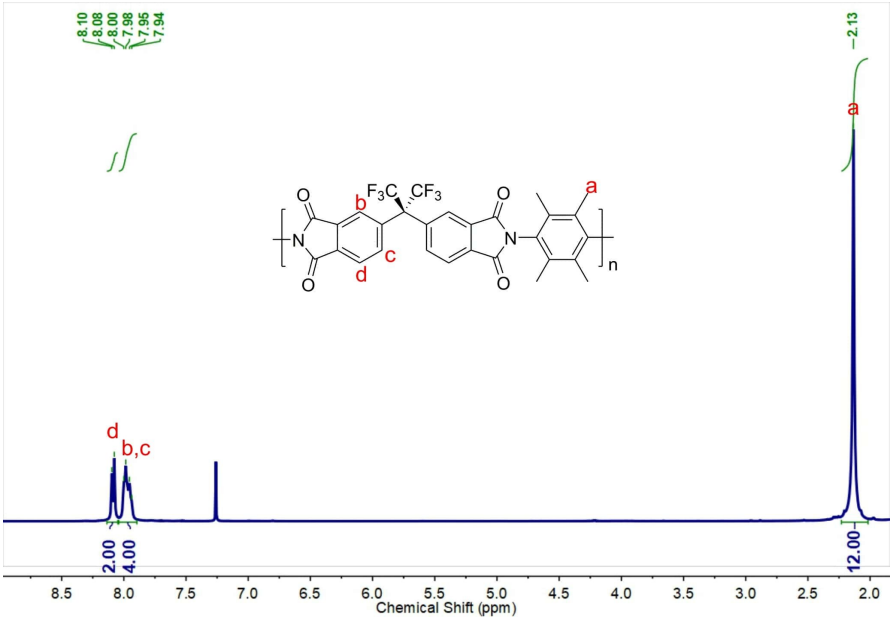

Figure S9. ^{1}H NMR spectrum of 6FDA-durene. The peak at 7.26 ppm corresponding to $CDCl_3$. ^{1}H NMR (400 MHz, $CDCl_3$), 8.08-8.10 (d, 2H), 7.94-8.01 (m, 4H),2.13 (s, 12H).

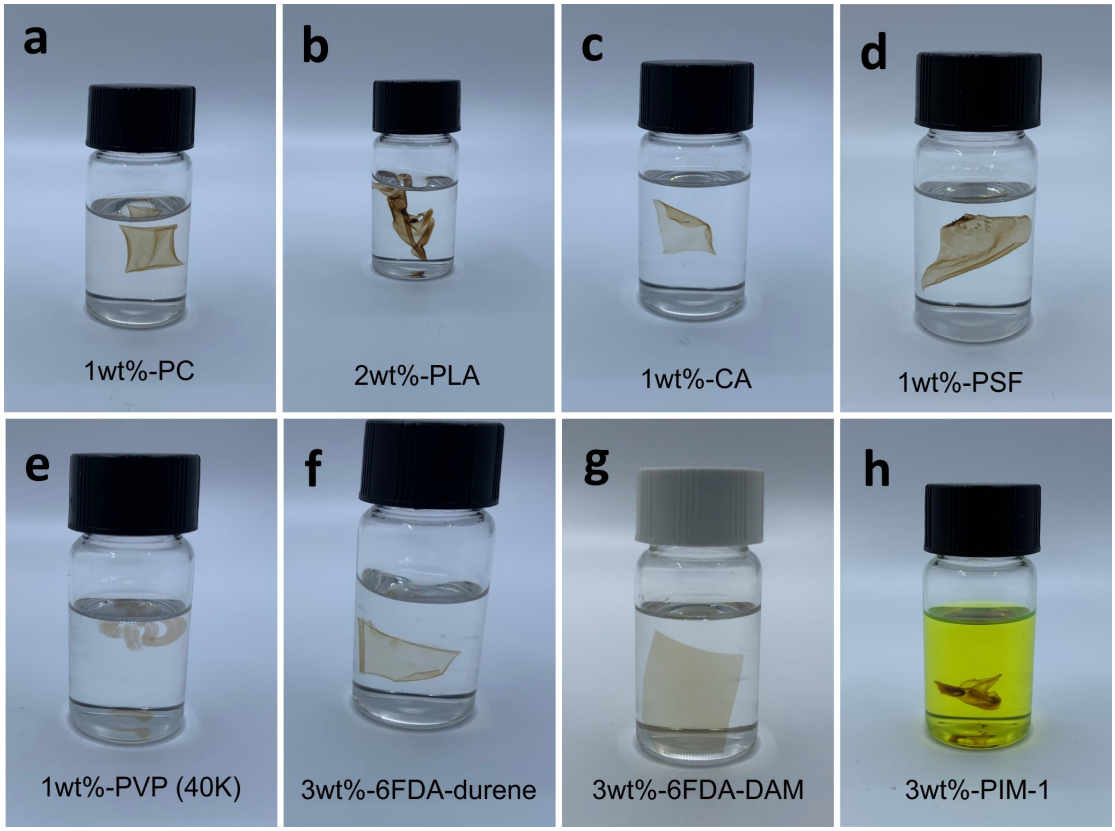

Figure S10. Photographs of various PgC_5Cu-polymer composite membranes immersed in DCM.

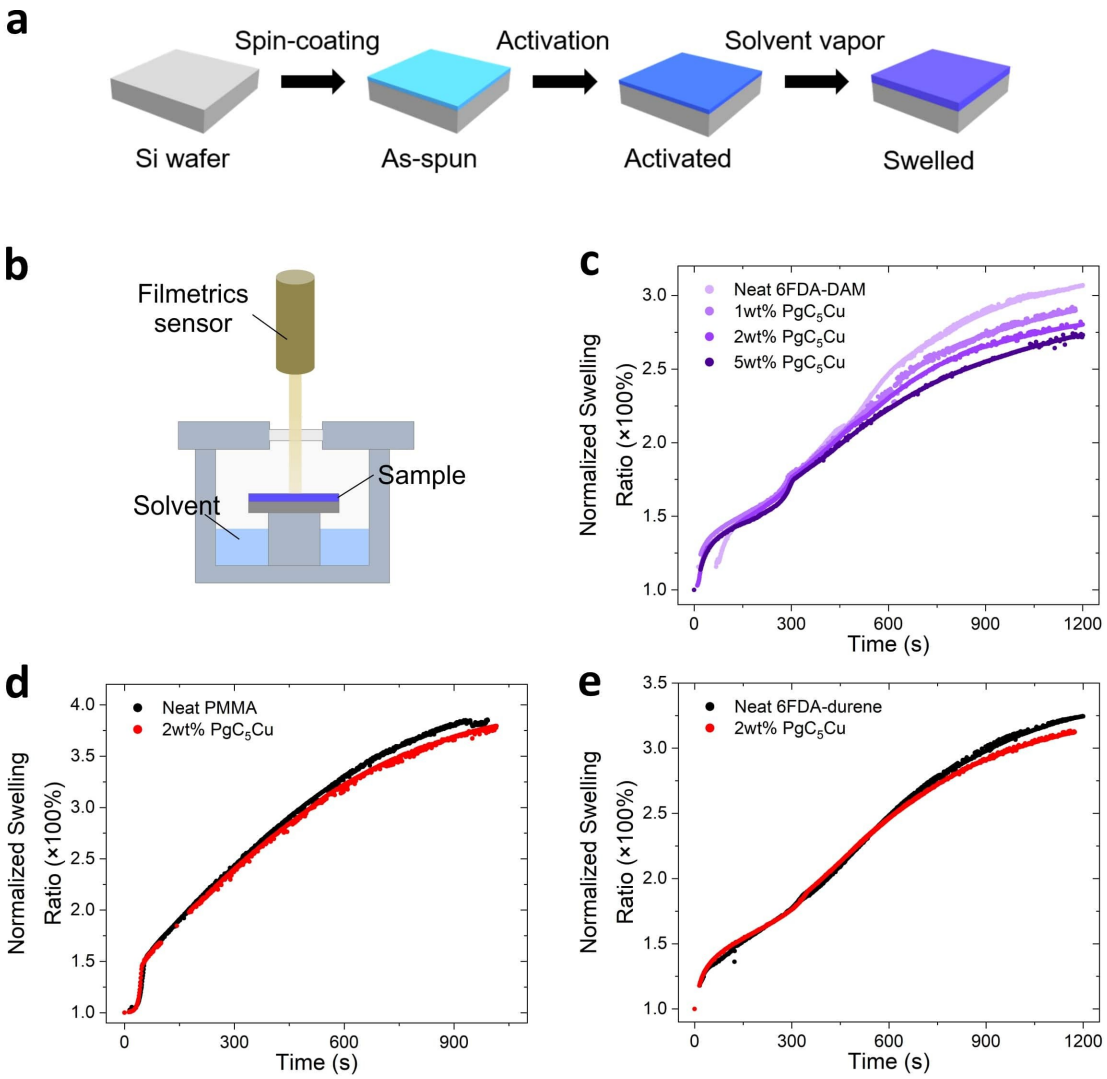

Figure S11. Schematic illustration of samples preparation (a) and measuring with an *in situ* film thickness monitor (b). Normalized swelling ratio change of 6FDA-DAM (c), PMMA (d) and 6FDA-durene (e) films after exposure to chloroform vapor for various time.

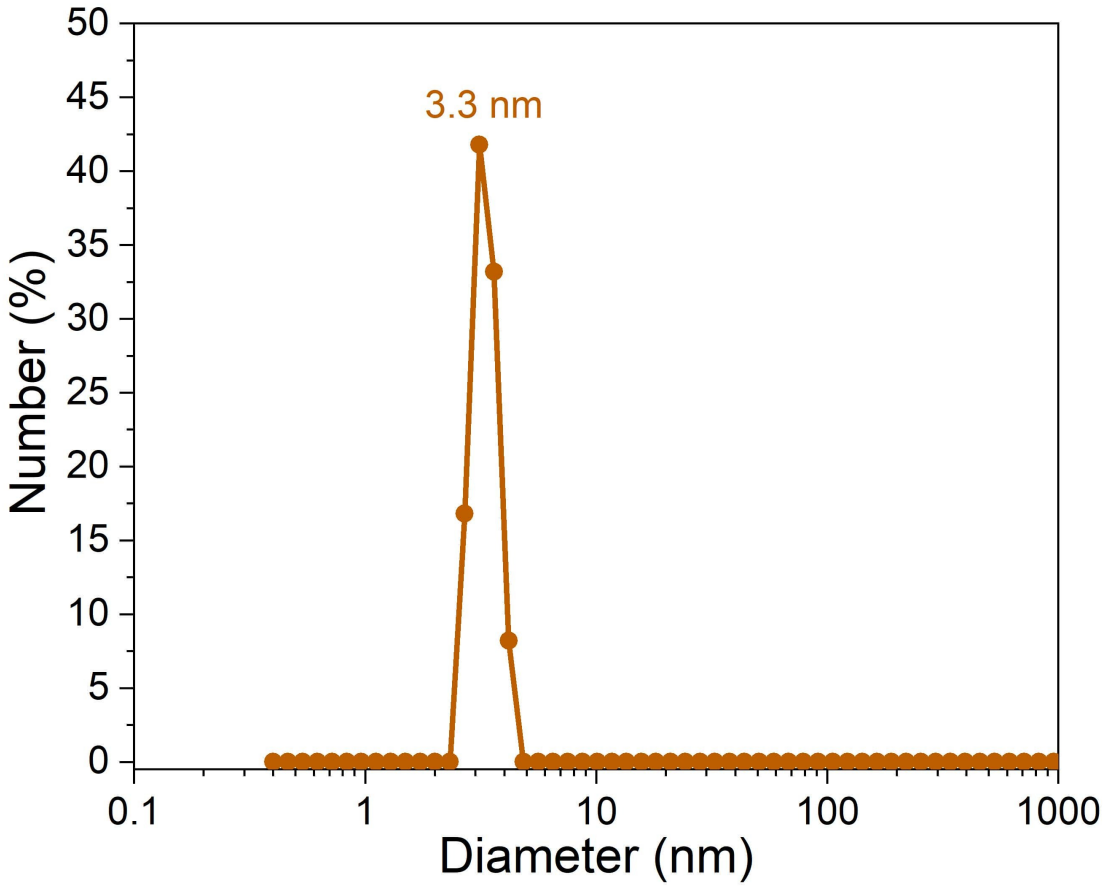

Figure S12. Hydrodynamic particle size distribution of a physical mixture of PgC_5Cu and PC in DCM measured by DLS.

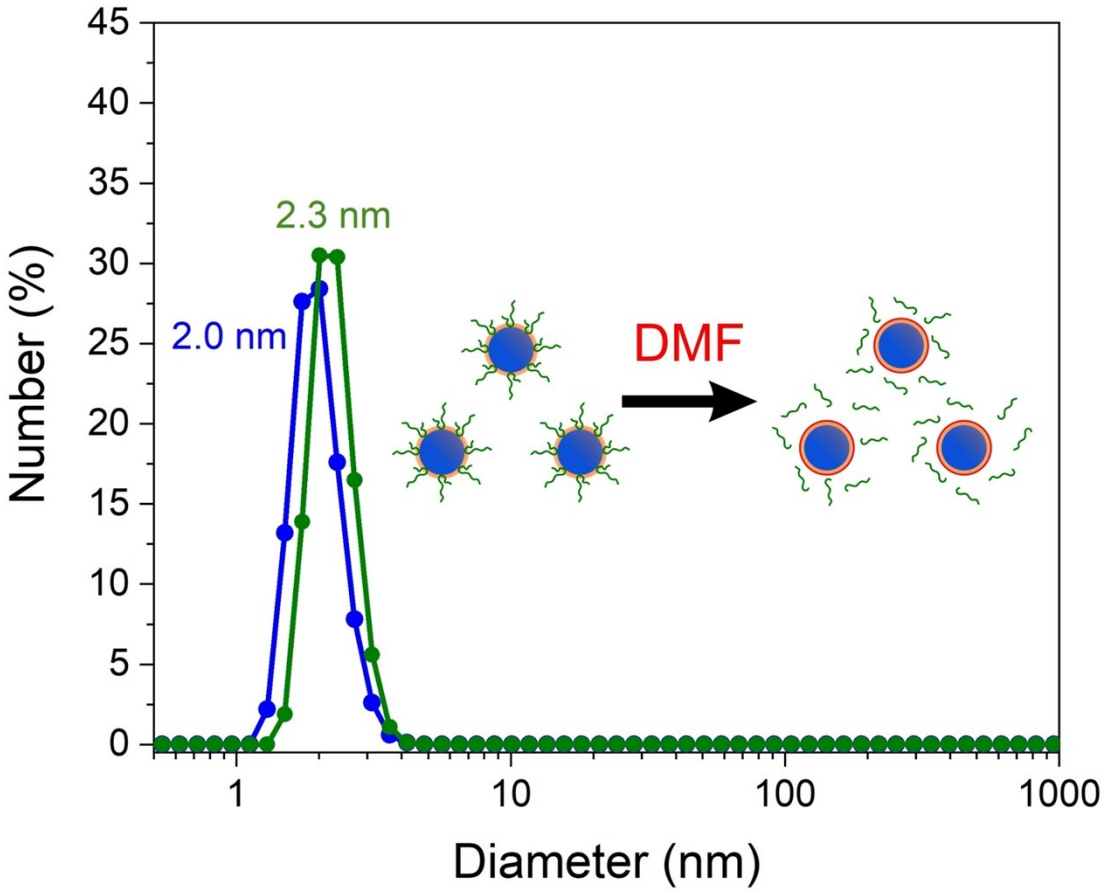

Figure S13. Hydrodynamic particle size distribution of a DMF solution of neat PgC_5Cu (blue) and a DMF solution of dissolved PC(1) membrane (green). Note that PC(1) does not fully dissolve in DMF at room temperature. Therefore, the dissolution was carried out at 120 ^{o}C. At such elevated temperature, the coordinately grafted PC chains were detached from the MONC surfaces and replaced by DMF molecules.

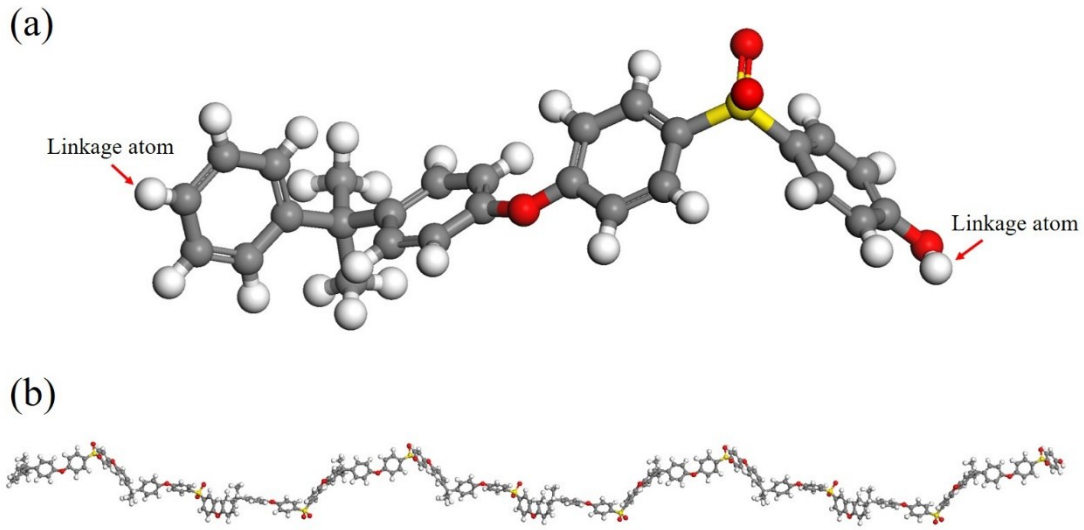

Figure S14. Atomic structure of (a) a phenylene sulfone repeating unit and (b) a random PSF polymer with 10 units.

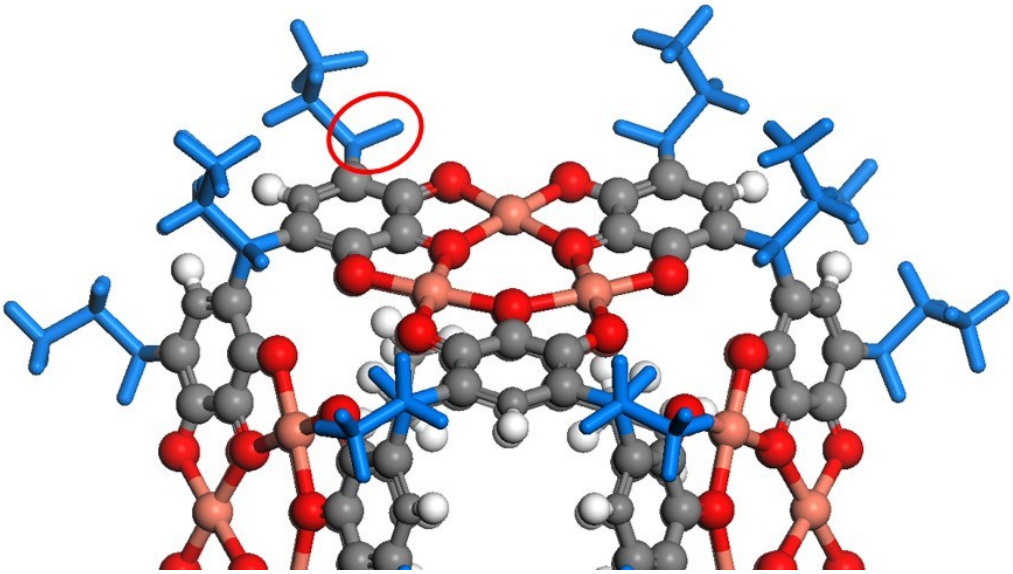

Figure S15. Alkyl part (shown as a light blue stick) and connections points (indicated as red circle) in PgC_3Cu. All other atoms are regarded as the non-alkyl part.

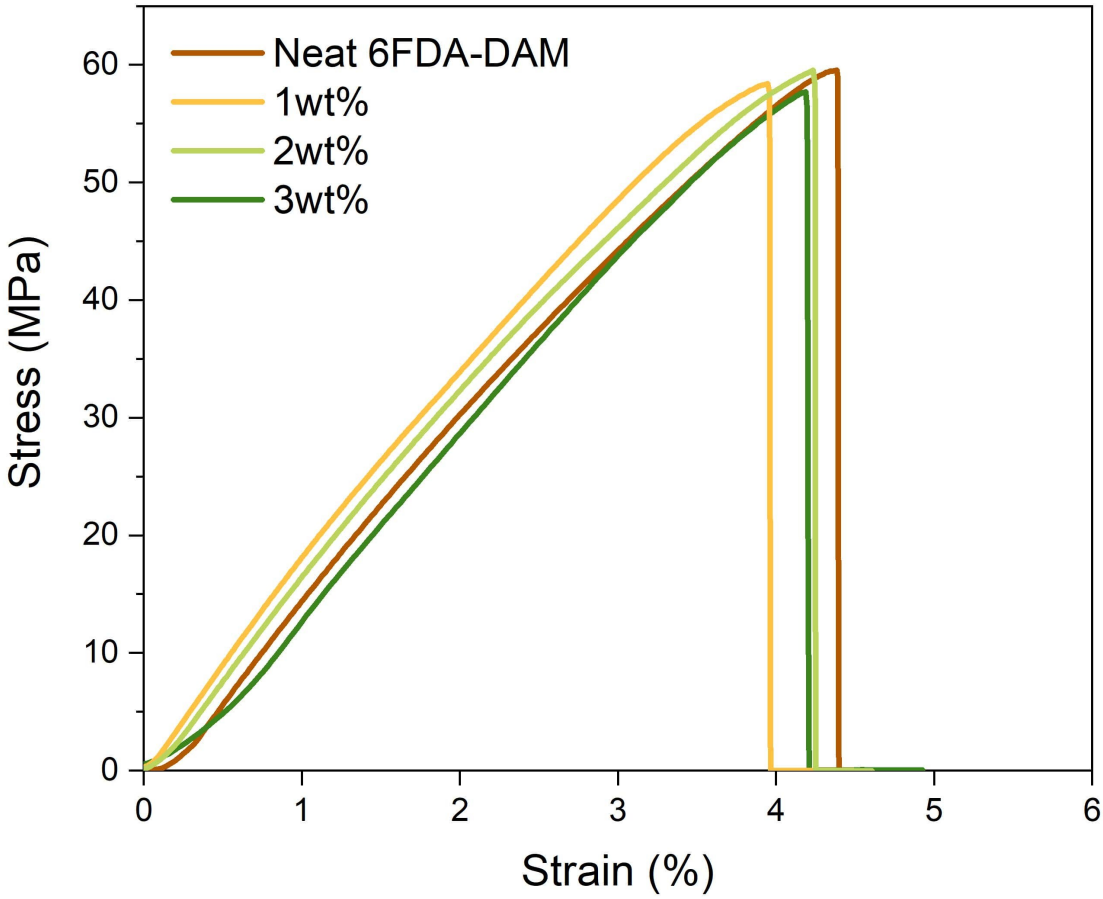

Figure S16. Stress – strain curves of neat 6FDA-DAM and its composite membranes containing PgC_5Cu.

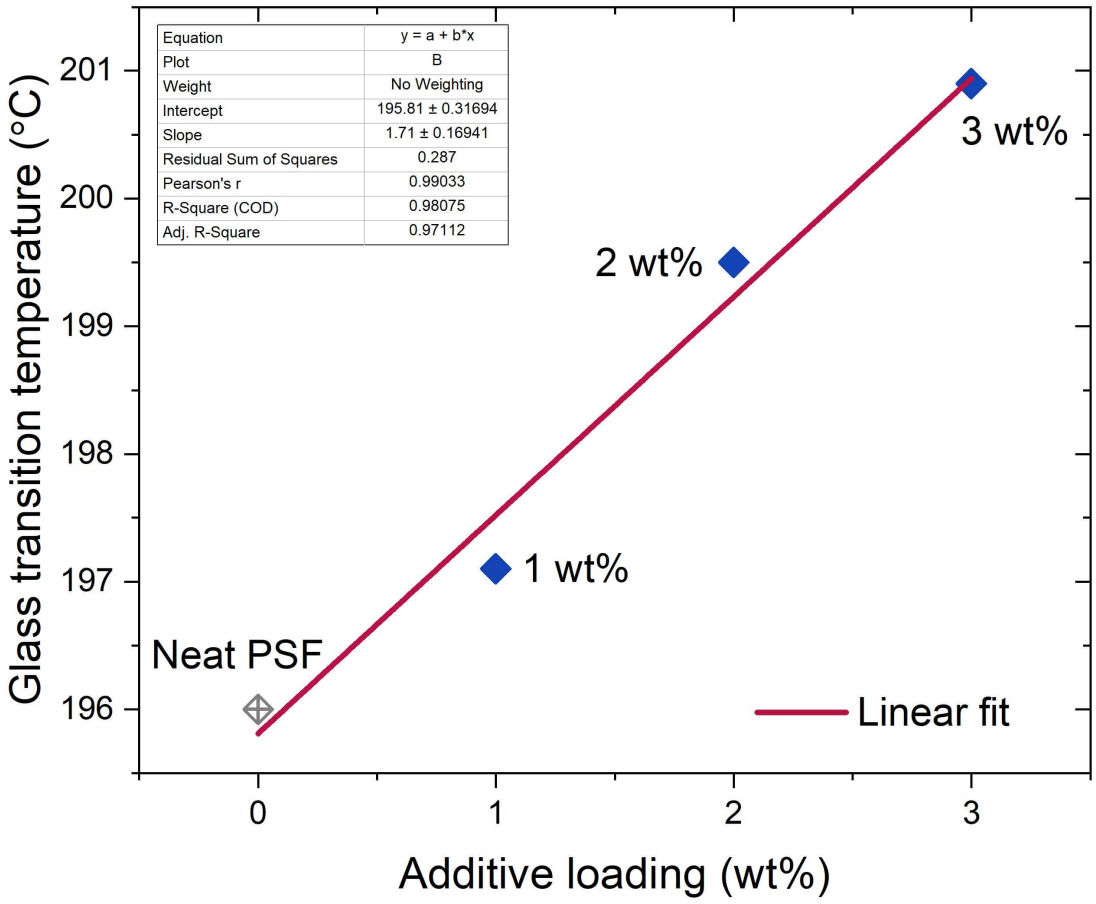

Figure S17. The relationship between glass transition temperature (T_g) and PgC_5C loading in PgC_5Cu-PSF composite membranes.

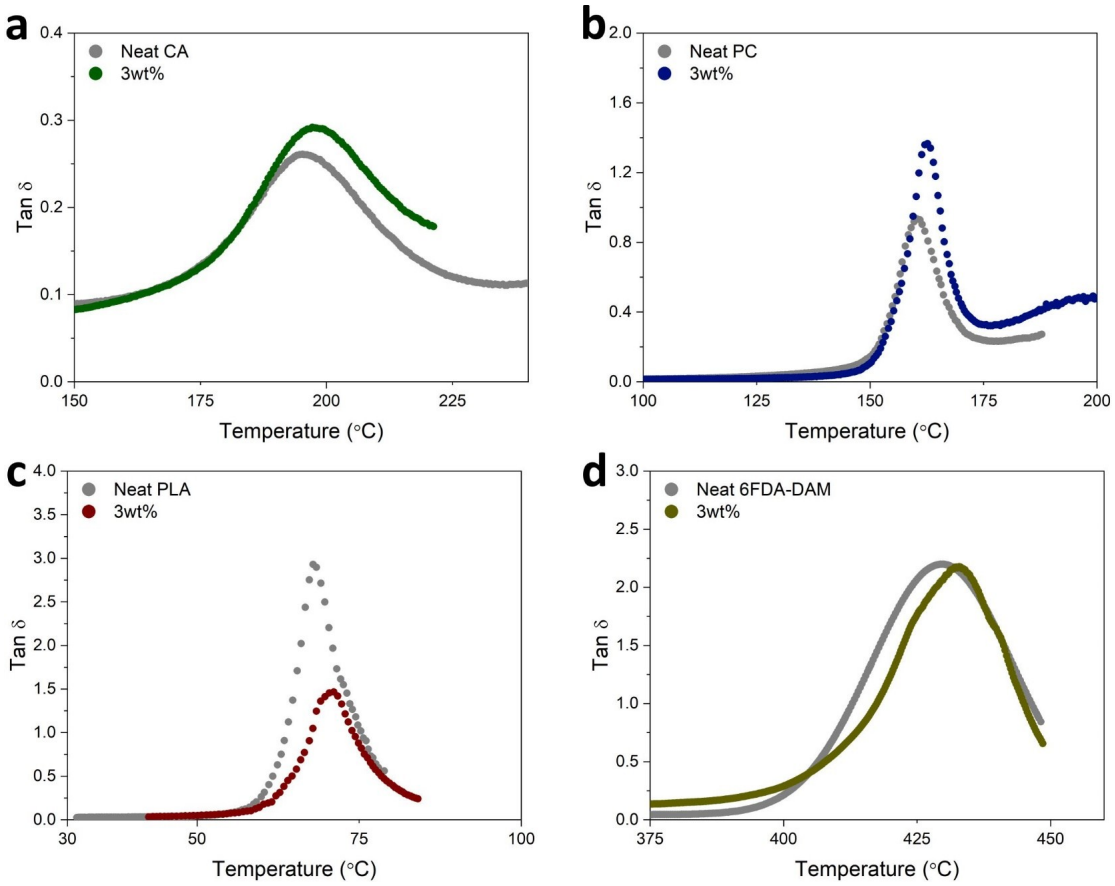

Figure S18. DMA plots showing tan δ of neat polymers and their composite membranes with respect to changing temperature.

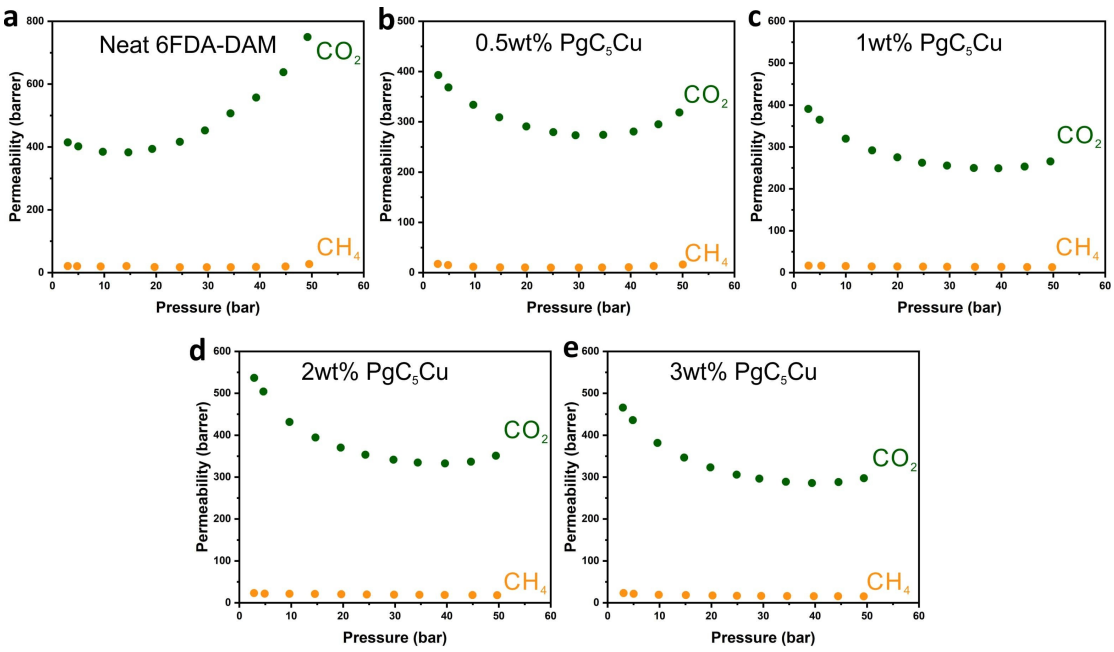

Figure S19. Pressure dependent CH_4 and CO_2 permeability change for neat 6FDA-DAM and their composite membranes.

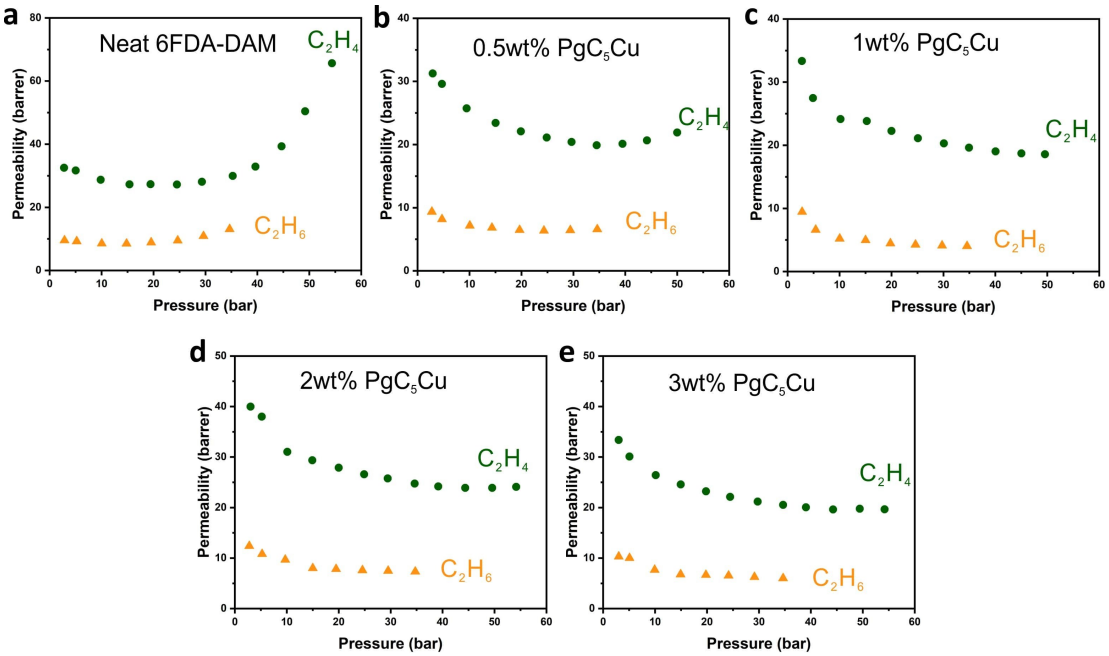

Figure S20. Pressure dependent C_2H_6 and C_2H_4 permeability change for neat 6FDA-DAM and their composite membranes.

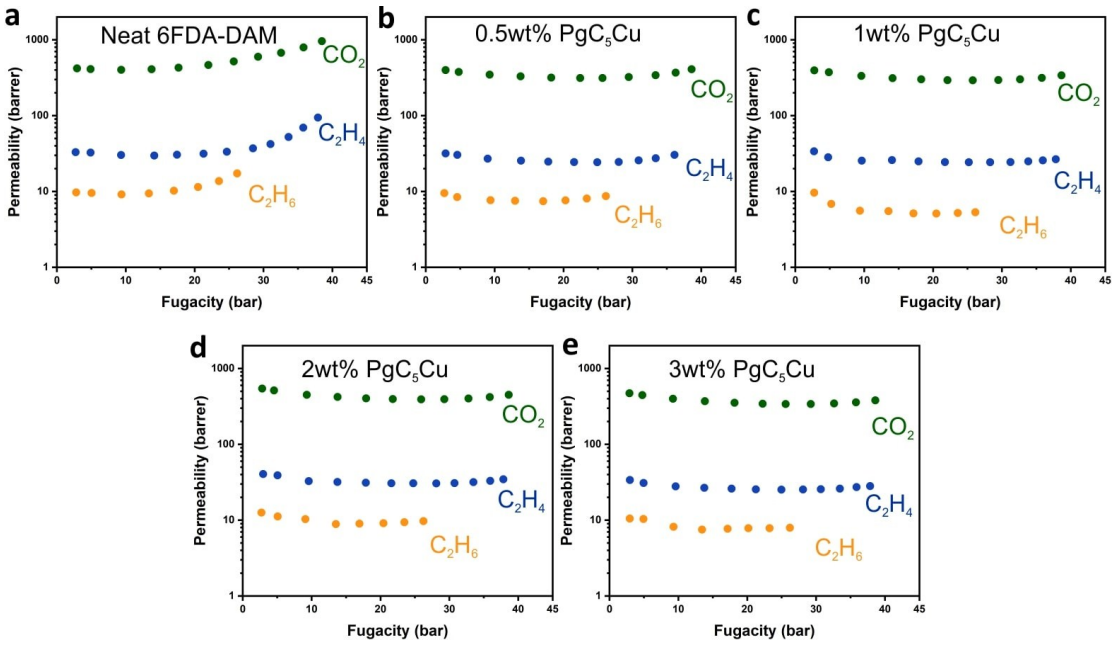

Figure S21. Feed fugacity dependent CO_2, C_2H_6 and C_2H_4 permeability change for neat 6FDA-DAM and their composite membranes.

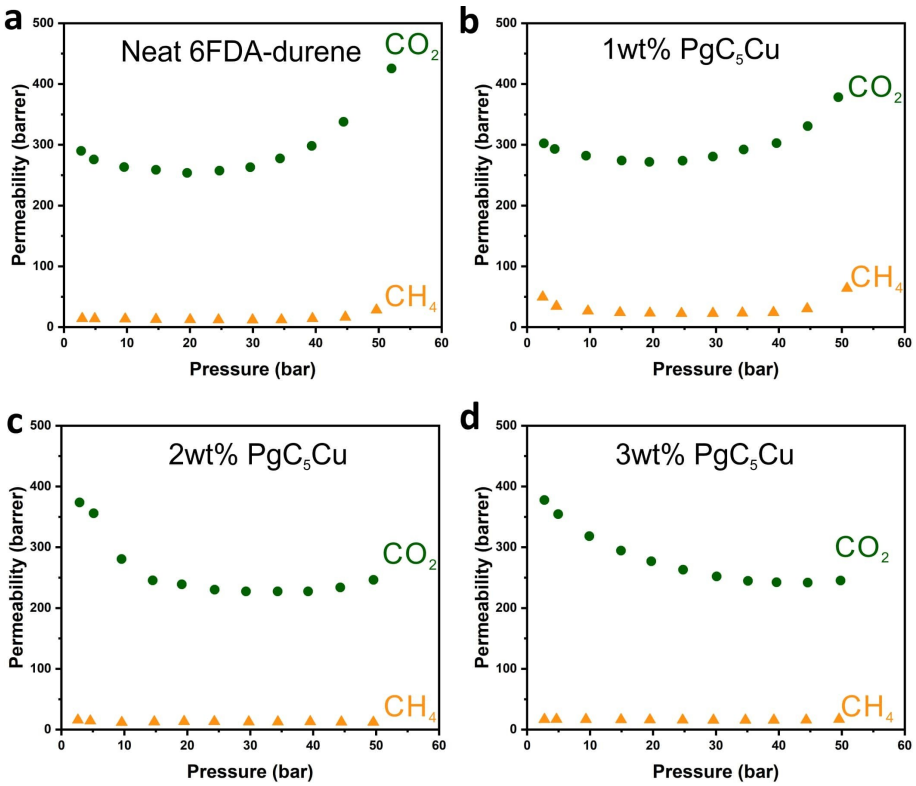

Figure S22. Pressure dependent CH_4 and CO_2 permeability change for neat 6FDA-durene and their composite membranes.

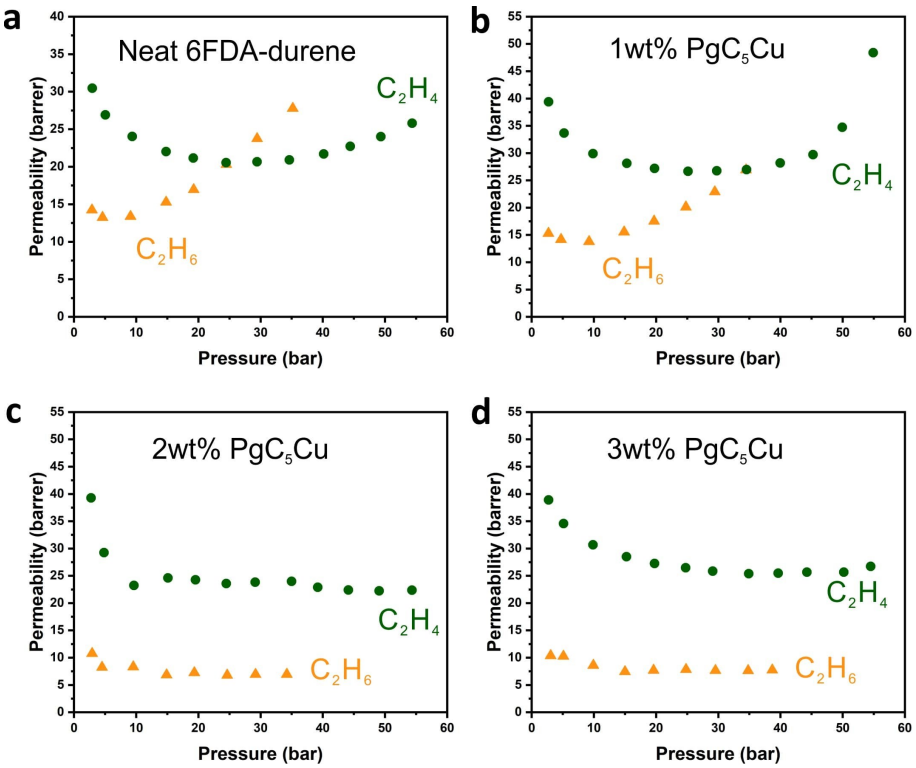

Figure S23. Pressure dependent C_2H_6 and C_2H_4 permeability change for neat 6FDA-durene and their composite membranes.

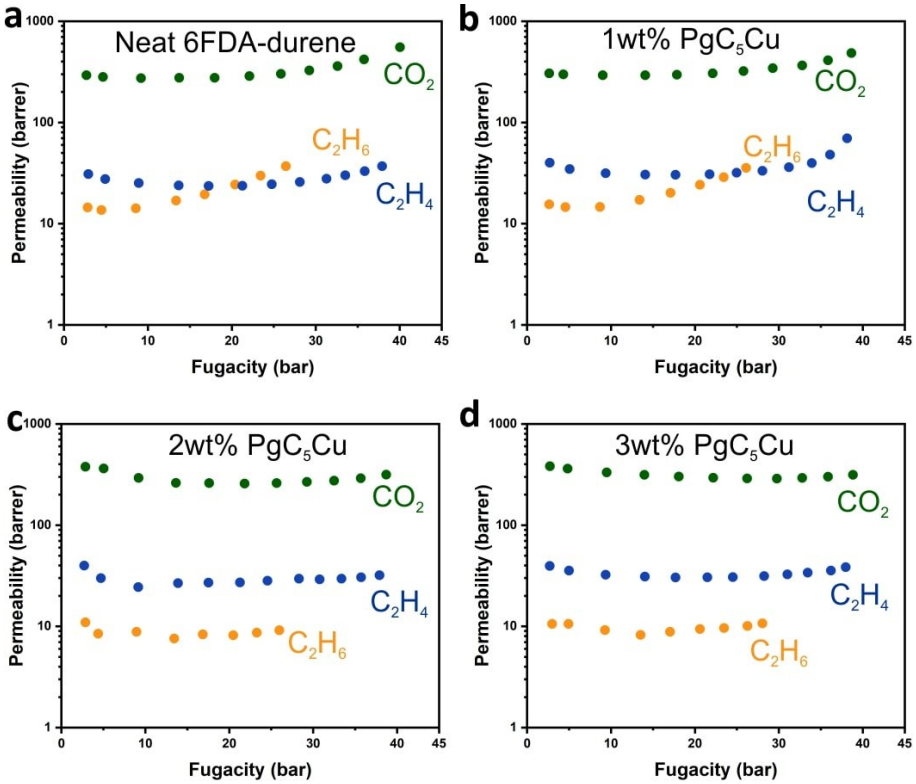

Figure S24. Feed fugacity dependent CO_2, C_2H_6 and C_2H_4 permeability change for neat 6FDA-durene and their composite membranes.

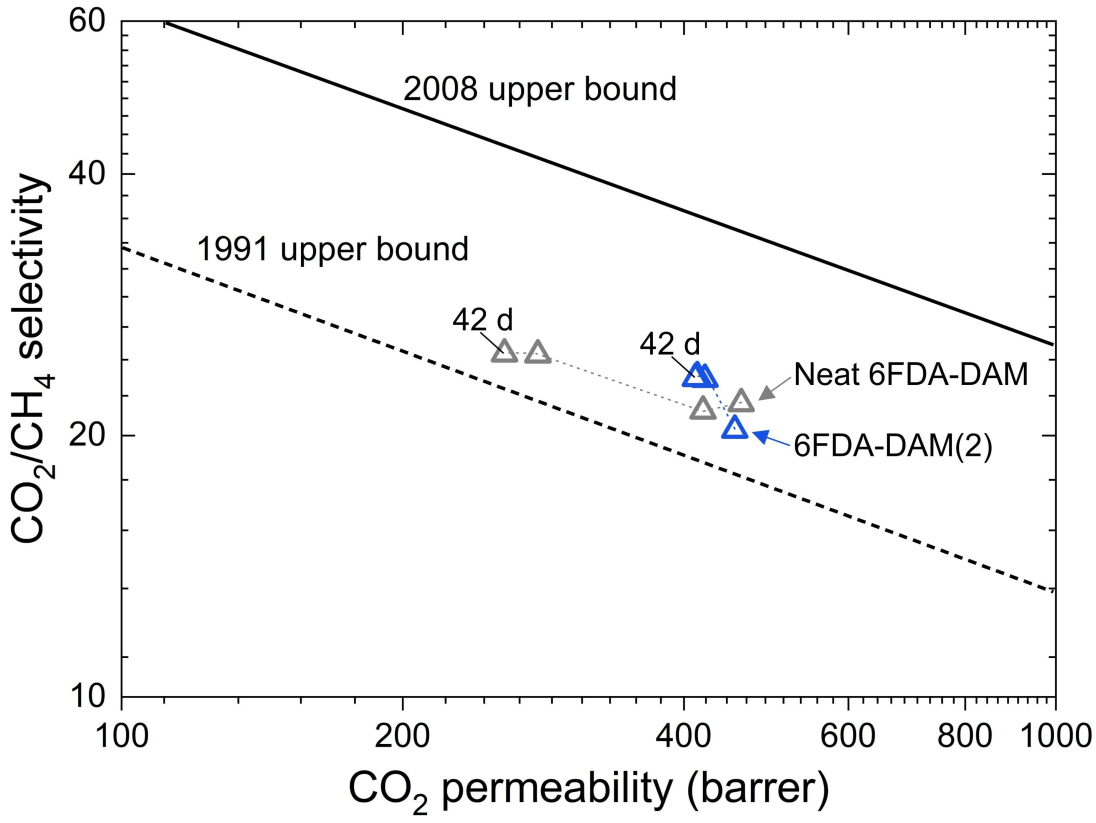

Figure S25. CO_2 permeability and CO_2/CH_4 selectivity of neat 6FDA-DAM (grey) and 6FDA-DAM(2) (blue) after various amount of time of physical aging.

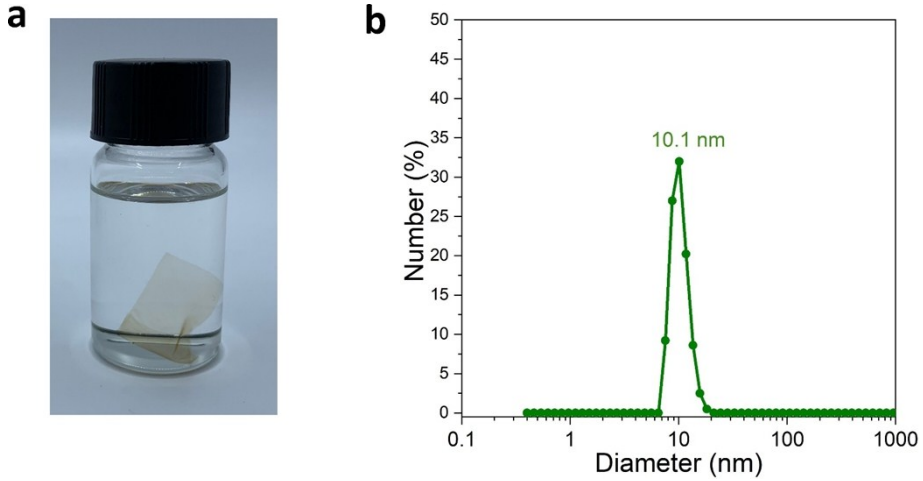

Figure S26. Long-term stability of the composite membranes. After thermal triggering, the 6FDA-DAM(1) membrane was stored under air environment with a relative humidity around 73% for 266 days. (a) A photograph of a piece of 6FDA-DAM(1) membrane immersed in DCM. (b) Hydrodynamic particle size distribution of a DCM solution of dissolved 6FDA-DAM(1) films by DLS.

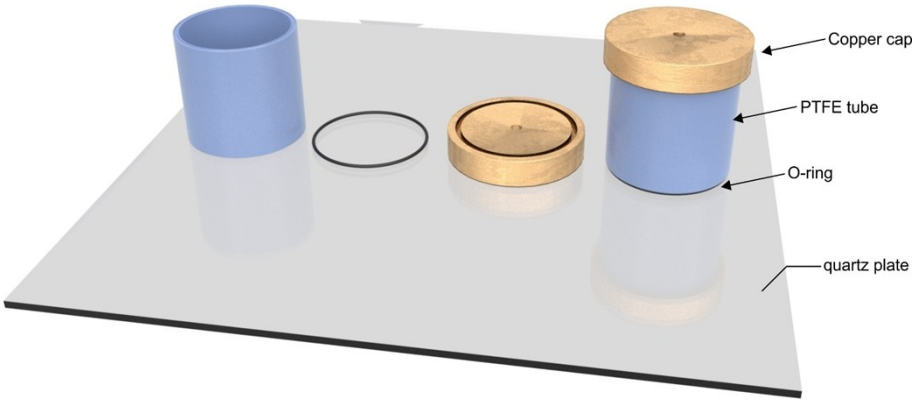

Scheme S1. Schematic diagram of a home-built membrane solution casting setup.

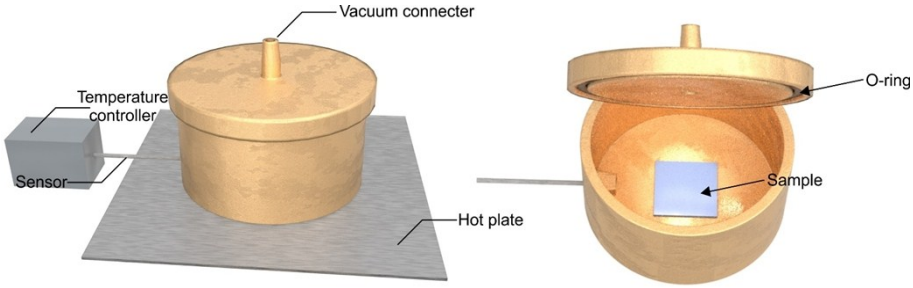

Scheme S2. Schematic diagram of a home-built membrane activation setup.

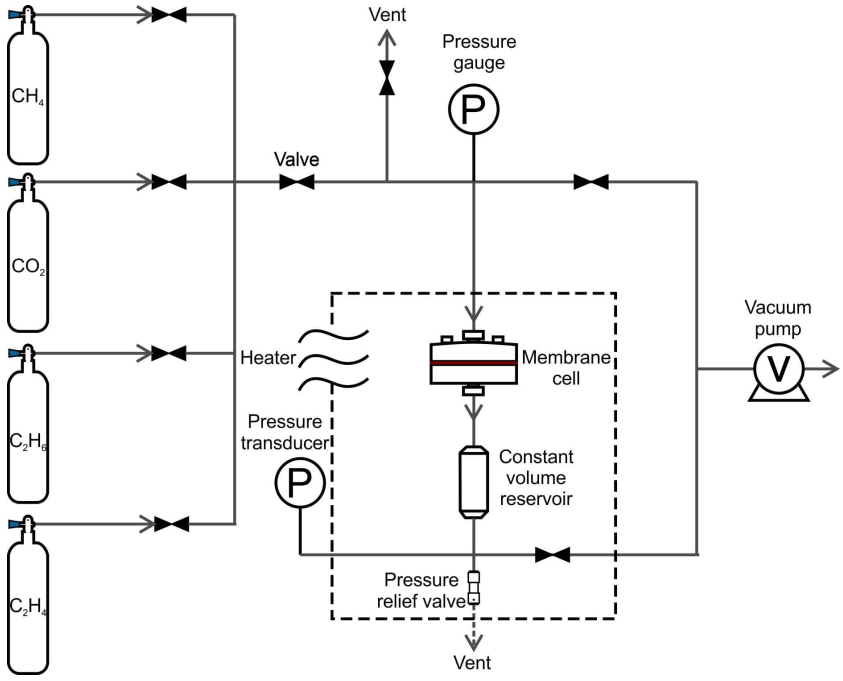

Scheme S3. Schematic diagram of a home-built constant volume variable pressure pure gas permeation setup.

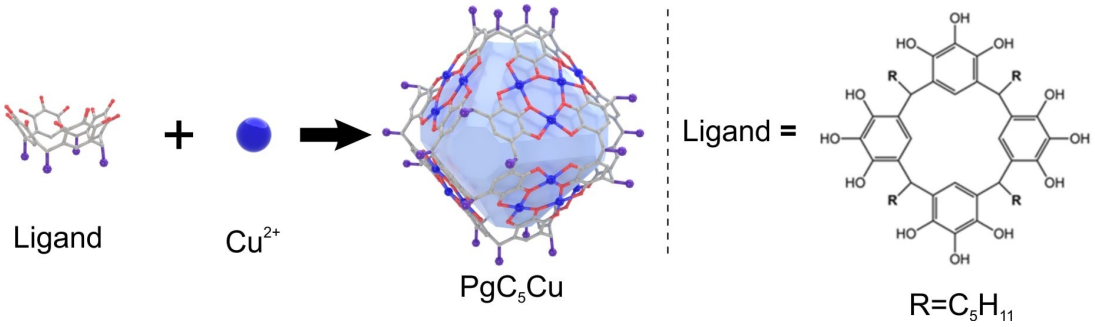

Scheme S4. Schematic diagram of synthesis of PgC_5Cu was shown, together with chemical structure of PgC_5 ligand.

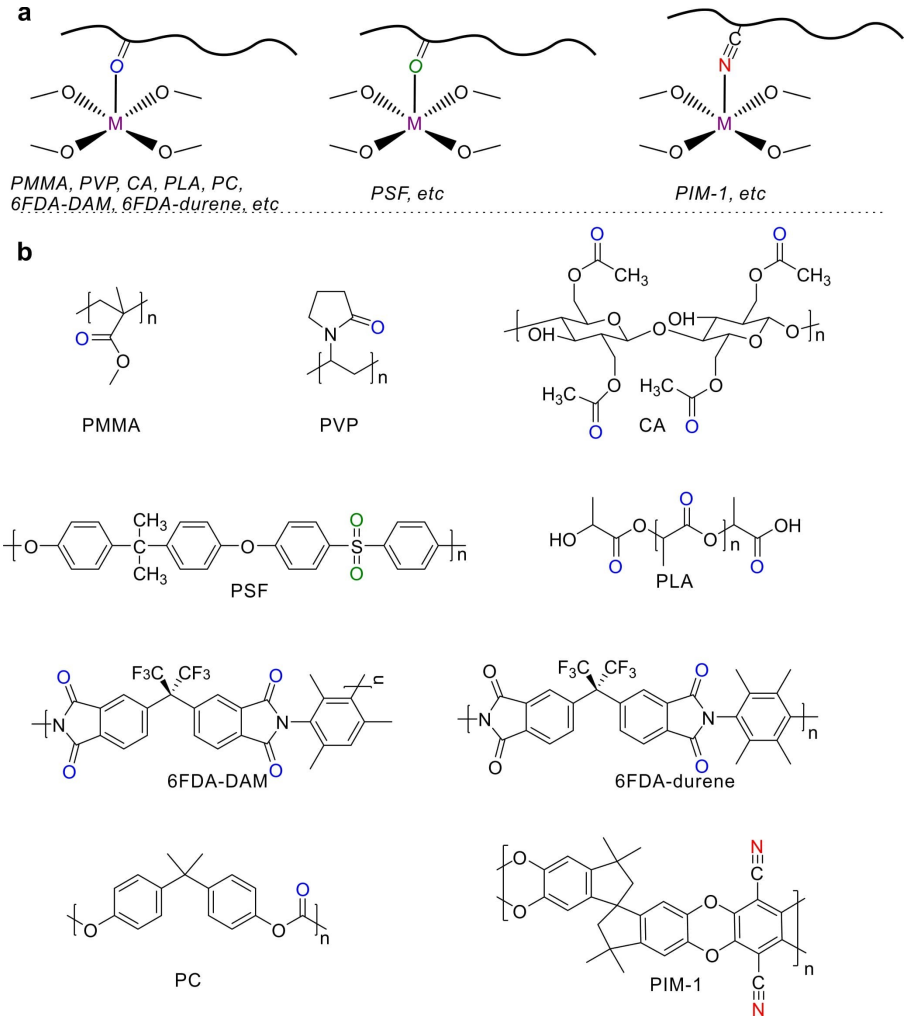

Scheme S5. Schematic drawing of (a) possible coordination bonds in MONC containing composite membranes and (b) the structures of polymers used in this work.

Tables

Table S1. Solubility of PgC_nCu nanocapsules in various solvents at room temperature. Note: - insoluble; ± slightly soluble; + soluble; ++ very soluble.

	Solvents			
MONCs	DCM	$CHCl_3$	DMF	MeOH
PgC_3Cu	-	-	±	±
PgC_5Cu	+	+	+	±
PgC_7Cu	++	++	+	±
PgC_9Cu	++	++	+	±

Table S2. Activation conditions for various neat polymer and PgC_5Cu-polymer composites used for various characterizations.

		Activation conditions	
Characterizations	Membranes or thin films	Temp. ºC	Time (h)
Swelling tests	PSF, PSF(0.5, 1.5, 2)	200	12
	PMMA, PMMA(2)	200	12
	6FDA-DAM, 6FDA-DAM(1, 2, 5)	250	12
	6FDA-durene, 6FDA-durene(2)	250	12
THF adsorption	6FDA-DAM(33)	230	12
Dissolution tests	PC(1, 2, 3)	200	12
FTIR	PMMA(50)	200	3
Mechanical properties	6FDA-DAM, 6FDA-DAM(1, 2, 3)	250	12
DMA	PSF, PSF(1, 2, 3)	250	2
	PLA, PLA(3)	200	3
	PC, PC(3)	200	3
	CA, CA(3)	200	3
	6FDA-DAM, 6FDA-DAM(3)	250	12
Permeation tests	6FDA-DAM, 6FDA-DAM(0.5, 1, 2, 3)	250	12
	6FDA-durene, 6FDA-durene(1, 2, 3)	250	12
	CA, CA(3)	200	12
	PC, PC(3)	200	12

Table S3. Atom types and their charges of PSF

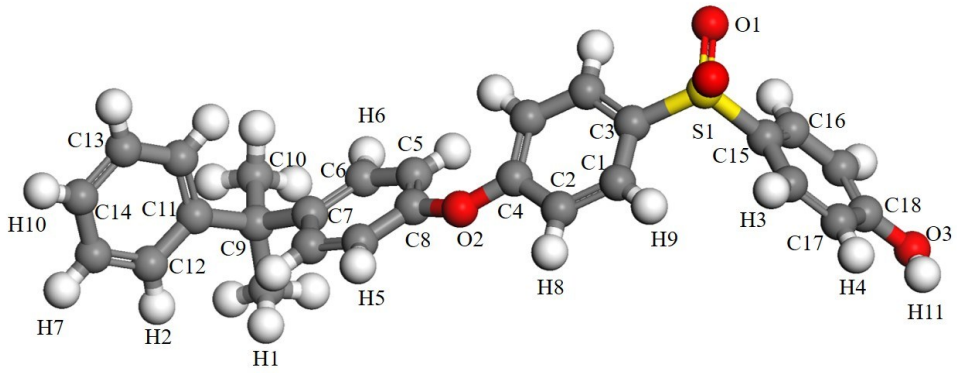

Atom type	Charge	Atom Type	Charge
H1	0.104861	C7	0.035946
H2	0.113081	C8 (in a monomer at edges)	0.414522
H3	0.163799	C9	0.273267
H4	0.163287	C10	-0.40351
H5	0.176007	C11	0.134262
H6	0.129816	C12	-0.1755
H7	0134619	C13	-0.15131
H8	0.155001	C14 (in a monomer at edges)	-0.12446
H9	0.159546	C15	-0.06227
H10	0.124939	C16	-0.15704
H11	0.36313	C17	-0.22117
S1	1.005979	C18 (in a monomer at edges)	0.350612
C1	-0.12148	O1	-0.5479
C2	-0.25077	O2	-0.39719
C3	-0.10404	O3	-0.50756
C4 (in a monomer at edges)	0.408959	C8 & C14 (in a mononer at mid-chain)	0.33387
C5	-0.30672	C4 & C18 (in a mononer at mid-chain)	0.33881
C6	-0.13242	O2 & O3 (in a mononer at mid-chain)	-0.32478

Table S4. Atom type and their charges for PgC_n.

Type	Charge	Type	Charge
Cu	0.9065	C2	0.6685
O1	-0.9788	C3	0.0005
O2	-0.9702	C4	-0.0334
C1	0.5403	H1	0.0205

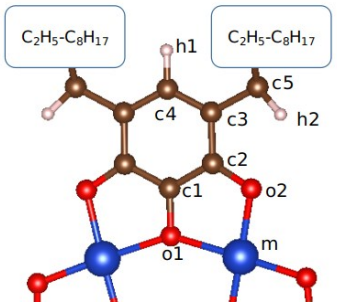

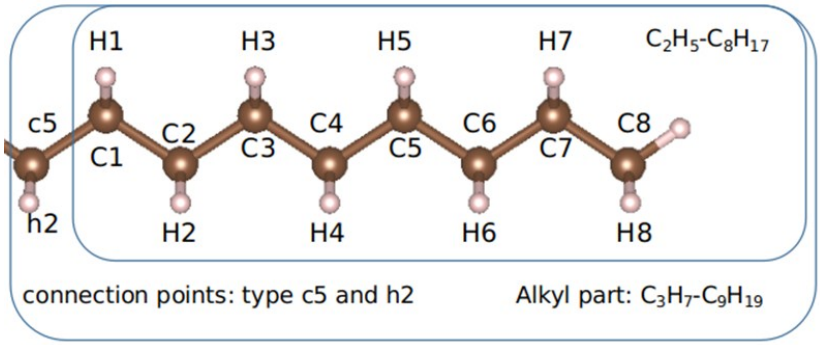

	C_nH_{2n+1} charges						
Type	C_2H_5	C_3H_7	C_4H_9	C_5H_{11}	C_6H_{13}	C_7H_{15}	C_8H_{17}
C1	0.28729	0.09661	0.13968	0.19844	0.16491	0.15687	0.17567
H1	-0.05559	-0.01030	-0.02741	-0.03843	-0.02915	-0.02910	-0.03293
C2	-0.22314	0.09661	-0.05132	-0.02568	0.03528	0.00034	-0.00493
H2	0.04502	-0.01030	0.00762	-0.00459	-0.01411	-0.00655	-0.00689
C3	\	-0.22592	0.13968	-0.02568	-0.02525	0.03840	0.00051
H3	\	0.04997	-0.02741	-0.00459	-0.01327	-0.02227	-0.01438
C4	\	\	-0.18614	0.19844	0.03528	0.03840	0.11008
H4	\	\	0.03977	-0.03843	-0.01411	-0.02227	-0.03332
C5	\	\	\	-0.23268	0.16491	0.00034	0.00051
H5	\	\	\	0.04866	-0.02915	-0.00655	-0.01438
C6	\	\	\	\	-0.24520	0.15687	-0.00493
H6	\	\	\	\	0.05247	-0.02910	-0.00689
C7	\	\	\	\	\	-0.22057	0.17567
H7	\	\	\	\	\	0.04694	-0.03293
C8	\	\	\	\	\	\	-0.23179
H8	\	\	\	\	\	\	0.04908
C5	-0.05437	-0.04727	-0.02788	-0.05664	-0.06154	-0.04798	-0.05491
H2	0.06873	0.06873	0.06873	0.06873	0.06873	0.06873	0.06873

Table S5. The change of CO_2/CH_4 separation performance for neat 6FDA-DAM and 6FDA-DAM(2) over time.

Membranes	Thickness (μm)	Aging days	Permeability (barrer) & Selectivity	
			CO_2	CO_2/CH_4
Neat 6FDA-DAM (MeOH treated)	54	As-cast	461	21.8
		14	419	21.4
		28	279	24.8
		42	257	24.8
6FDA-DAM(2) (MeOH treated)	53	As-cast	453	20.3
		14	421	23.2
		28	413	23.4
		42	411	23.3

References

1 C. Zhang, R. S. Patil, T. Li, C. L. Barnes, S. J. Teat and J. L. Atwood, *Chem. – Eur. J*, 2017, **23**, 8520-8524.
2 J. E. Bachman, Z. P. Smith, T. Li, T. Xu and J. R. Long, *Nat. Mater.*, 2016, **15**, 845-849.
3 J. Song, N. Du, Y. Dai, G. P. Robertson, M. D. Guiver, S. Thomas and I. Pinnau, *Macromolecules*, 2008, **41**, 7411-7417.
4 S. Zhang, J. Li, J. Zhao, D. Wu, B. Yuan, W. Y. Hernández, W. Zhou, T. He, Y. Yu, Y. Yang, V. Ordomsky, T. Li. *Nano Res*., just accepted.
5 Accelrys Software Inc., Discovery Studio Modeling Environment, Release x.x , San Diego: Accelrys Software Inc. 2007.
6 C. I. Bayly, P. Cieplak, W. Cornell and P. A. Kollman, *J. Phys. Chem.*, 1993, **97**, 10269-10280.
7 M. J. Frisch, G. W. Trucks, H. B. Schlegel, G. E. Scuseria, M. A. Robb, J. R. Cheeseman, G. Scalmani, V. Barone, B. Mennucci, G. A. Petersson, H. Nakatsuji, M. Caricato, X. Li, H. P. Hratchian, A. F. Izmaylov, J. Bloino, G. Zheng, J. L. Sonnenberg, M. Hada, M. Ehara, K. Toyota, R. Fukuda, J. Hasegawa, M. Ishida, T. Nakajima, Y. Honda, O. Kitao, H. Nakai, T. Vreven, J. A. Montgomery, Jr., J. E. Peralta, F. Ogliaro, M. Bearpark, J. J. Heyd, E. Brothers, K. N. Kudin, V. N. Staroverov, R. Kobayashi, J. Normand, K. Raghavachari, A. Rendell, J. C. Burant, S. S. Iyengar, J. Tomasi, M. Cossi, N. Rega, J. M. Millam, M. Klene, J. E. Knox, J. B. Cross, V. Bakken, C. Adamo, J. Jaramillo, R. Gomperts, R. E. Stratmann, O. Yazyev, A. J. Austin, R. Cammi, C. Pomelli, J. W. Ochterski, R. L. Martin, K. Morokuma, V. G. Zakrzewski, G. A. Voth, P. Salvador, J. J. Dannenberg, S. Dapprich, A. D. Daniels, Ö. Farkas, J. B. Foresman, J. V. Ortiz, J. Cioslowski, and D. J. Fox, Gaussian 09 (Gaussian, Inc., Wallingford CT, 2009)
8 J. P. Perdew, K. Burke and M. Ernzerhof, *Phys. Rev. Lett.*, 1996, **77**, 3865-3868.
9 G. Kresse and D. Joubert, *Phys. Rev. B*, 1999, **59**, 1758-1775.
10 P. E. Blochl, *Phys. Rev. B*, 1994, **50**, 17953-17979.
11 W. Tang, E. Sanville and G. Henkelman, *J. Phys.: Condens. Matter*, 2009, **21**, 1-7.
12 S. Plimpton, *J. Comput. Phys.*, 1995, **117**, 1-19.
13 J. Wang, R. M. Wolf, J. W. Caldwell, P. A. Kollman and D. A. Case, *J. Comput. Chem.*, 2004, **25**, 1157-1174.
14 S. M. Woodley, P. D. Battle, J. D. Gale and C. Richard A. Catlow, *Phys. Chem. Chem. Phys.*, 1999, **1**, 2535-2542.
15 J. H. Dymond, K. N. Marsh, R. C. Wilhoit, and K. C. Wong, The virial coefficients of pure gases and mixtures, Oxford Univ. Press, 2001.
16 L. M. Robeson, *J. Membr. Sci.*, 1991, **62**, 165-185.
17 L. M. Robeson, *J. Membr. Sci.*, 2008, **320**, 390-400.
18 M. Rungta, C. Zhang, W. J. Koros and L. Xu, *AlChE J.*, 2013, **59**, 3475-3489.